Supporting information for:

Dysprosium-Modified Tobacco Mosaic Virus Nanoparticles for Ultra-High-Field Magnetic Resonance and Near-Infrared Fluorescence Imaging of Prostate Cancer

He Hu[a], Yifan Zhang[a], Sourabh Shukla[a], Yuning Gu[a], Xin Yu[a] and Nicole F. Steinmetz*[a,b,c,d,e]

[a] Department of Biomedical Engineering, Case Western Reserve University Schools of Medicine and Engineering, 10900 Euclid Ave., Cleveland, OH 44106, USA

[b] Department of Radiology, Case Western Reserve University School of Medicine, 10900 Euclid Ave., Cleveland, OH 44106, USA

[c] Department of Materials Science and Engineering, Case Western Reserve University School of Engineering, 10900 Euclid Ave., Cleveland, OH 44106, USA

[d] Department of Macromolecular Science and Engineering, Case Western Reserve University School of Engineering, 10900 Euclid Ave., Cleveland, OH 44106, USA

[e] Division of General Medical Sciences-Oncology, Case Western Reserve University, 10900 Euclid Ave., Cleveland, OH 44106, USA

*Corresponding author: nicole.steinmetz@case.edu

Synthesis and Characterization of Dy(DOTA)-azide:

DOTA-azide was dissolved in water (~ 10 mg/mL) with 1.2 eq of $DyCl_3 \bullet 6H_2O$, the pH of the solution was adjusted to ~5.0 by the addition of aqueous 1.0 M NaOH solution (Figure S1A). The reaction mixture was stirred at room temperature and the pH was monitored every 3~4 hours and kept at pH ~5.0. Then pH was brought to ~7.0 and the solution was stirred for an additional 30 min. The reaction mixture was then centrifuged at 9000 rpm for 10 min to remove precipitate. The supernatant was freeze-dried to give the product as hygroscopic white powder. The raw DOTA-azide and final Dy-DOTA-azide samples were characterized by MALDI-TOF (Bruker AutoFlex III MALDI-TOF-TOF MS) as shown in Figure S1 B and C, respectively.

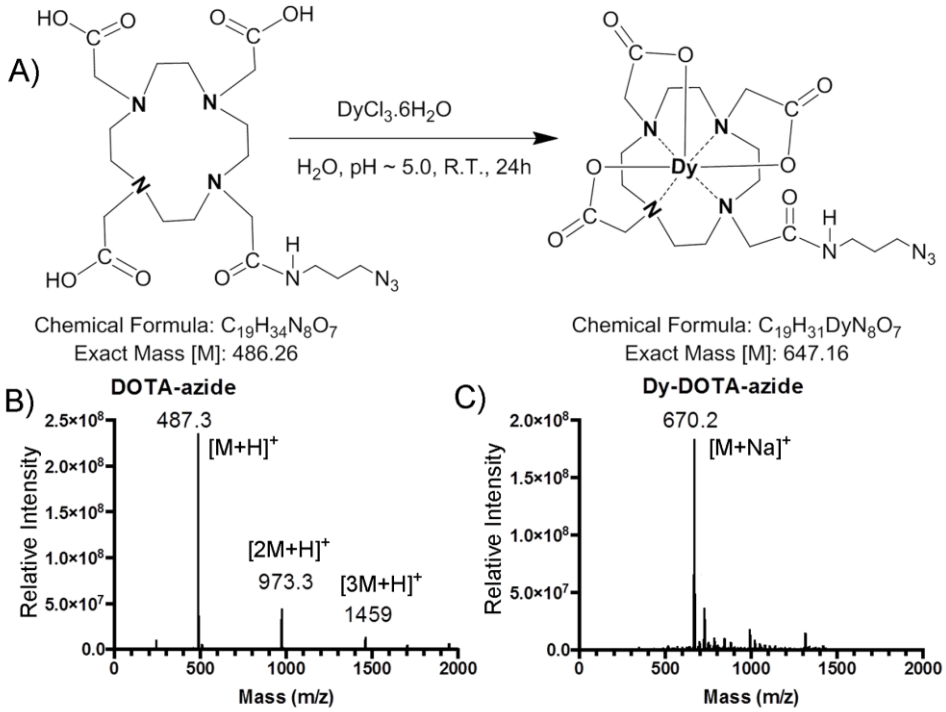

Figure S1. (A) Scheme showing the synthesis of Dy-DOTA-azide. MALDI-TOF mass spectra of DOTA-azide (B) and final Dy-DOTA-azide (C) samples.

TMV bioconjugation procedures

Internal surface modification with Dy(DOTA) and Cy7.5

The TMV interior was labeled with terminal alkynes, targeting the carboxylate side chains of glutamic acid residues 97 and 106. Purified TMV particles were mixed with 100 molar equivalents per coat protein (Eq/CP) of propargyl amine (Sigma-Aldrich, St. Louis, MO, USA), 50 Eq/CP of ethyldimethylaminopropylcarbodiimide (EDC) (Sigma-Aldrich) and 10 Eq/CP of n-hydroxybenzotriazole (Sigma-Aldrich) in 100 mM HEPES buffer (pH 7.0) for 24 h at room temperature. The resulting product (iAlk-TMV) was purified by sucrose cushion ultracentrifugation (1.5 mL 40% sucrose cushion, 42,000 rpm using a Ti50.2 rotor, 3 h). Dy(DOTA)-azide and Cy7.5-azide were attached to iAlk-TMV using the copper-catalyzed azide-alkyne cycloaddition (CuAAC) reaction. Cy7.5-azide was purchased from Lumiprobe Corp. (Hallandale Beach, FL, USA) whereas Dy(DOTA)-azide was prepared in-house by incubating $DyCl_3$ (Sigma-Aldrich) with azidomono-amide-1,4,7,10-tetraazacyclododecane-N,N',N'',N'''-tetraacetic acid (Macrocyclics, Plano, TX, USA) for 24 h while maintaining the pH at 6 – 7 by periodic adjustment with 1 M NaOH, followed by freeze drying to produce Dy(DOTA)-azide powder. The iAlk-TMV was mixed with 5 Eq/CP of Dy(DOTA)-azide and 0.2 Eq/CP of Cy7.5-azide in the presence of 1 mM $CuSO_4$, 2 mM aminoguanidine and 2 mM ascorbic acid in 10 mM phosphate buffer (pH 7.0) for 30 min on ice. The resulting Dy-Cy7.5-TMV particles were purified by sucrose gradient ultracentrifugation as above, and the pellet was dispersed in PBS (pH 7.0).

External surface modification with PEG and DGEA

The exterior of the Dy-Cy7.5-TMV particles was labeled with terminal alkynes by

targeting the tyrosine 139 residues. Dy-Cy7.5-TMV was mixed with 25 Eq/CP of in situ generated diazonium salt (3-ethynylaniline mixed with acidic sodium nitrite) in 100 mM borate buffer (pH 8.8) for 30 min on ice. The resulting Dy-Cy7.5-TMV-eAlk particles were purified by sucrose cushion ultracentrifugation as above and then externally conjugated to polyethylene glycol (PEG) with or without the peptide DGEA using the CuAAC reaction described above. For the control particles, the reaction was carried out with 10 Eq/CP polyethylene glycol succinimidyl ester (mPEG-NHS, 2000 Da; Nanocs Inc., New York, NY, USA) to generate the product Dy-Cy7.5-TMV-mPEG. For the targeted particles, the reaction was carried out with 10 Eq/CP azide polyethylene glycol maleimide (N_3-PEG-Mal, MW 2000 Da; Nanocs Inc.) to generate an intermediate that was centrifuged as above and redispersed in 10 mM phosphate buffer (pH 6.5) before reacting with 0.5 Eq/CP DGEA-cys for 3 h at room temperature. An excess of ethanethiol was added and the reaction incubated for a further 2 h to block the PEG maleimide group. The final Dy-Cy7.5-TMV-mPEG and Dy-Cy7.5-TMV-DGEA particles were dialyzed against PBS (pH 7.4) buffer for 4 h, concentrated and stored in PBS.

Size exclusion chromatography

The nanoparticle samples (100 µL of a 1.0 mg/mL solution) were analyzed by SEC using a Superose 6 column on the AKTA Explorer chromatography system (GE Healthcare, Little Chalfont, UK) at a flow rate of 0.5 mL/min in PBS (pH 7.4). The absorbance was then measured at 260 and 280 nm.

Transmission electron microscopy

A 20 µL aliquot of nanoparticle suspension was deposited onto a 300-mesh Formvar-carbon-coated copper grid (Electron Microscopy Sciences, Hatfield, Pam USA) and incubated at room temperature for 2 min. The grid was then stained with 20 µL 2% uranyl acetate (SPI Supplies, West Chester, PA, USA) and observed using a Tecnai F30 TEM system (FEI, Hillsboro, IR, USA).

SDS-PAGE and Western blot

Nanoparticle samples (20 µg) were denatured by boiling at 100 ^{o}C for 7 min in gel loading buffer (62.5 mM Tris-HCl (pH 6.8), 2% (w/v) SDS, 10% (v/v) glycerol, 0.01% (w/v) bromophenol blue, 10% (v/v) 2-mercaptoethanol). Denatured protein samples were then separated on 4–12% NuPAGE polyacrylamide gels (Pierce, Rockford, IL, USA) in 1 x MOPS running buffer at 200 V for 40 min. The gels were stained with Coomassie Brilliant Blue and visualized under white light using an AlphaImager imaging system (Protein Simple, San Jose, CA, USA). Samples separated by SDS-PAGE were transferred from the gel onto nitrocellulose membranes under a constant voltage of 30 V for 1 h. The membranes were blocked at room temperature for 1 h in TBST (150 mM NaCl,10 mM Tris-HCl, 0.1% (v/v) Tween-20, pH 7.5) containing 5% (w/v) skimmed milk and were then probed with the anti-PEG antibody PEG-2-128 (ab133471; Abcam, Cambridge, MA, USA) diluted 1:1000 in blocking solution, shaking overnight. After washing three times for 5 min in TBST, the membranes were incubated with an alkaline phosphatase-conjugated goat anti-rabbit

secondary antibody (Thermo Fisher Scientific) diluted 1:1000 in blocking solution, shaking for 30–60 min at room temperature. After washing again as above, followed by a final wash for 5 min in Millipore water, specific antibody binding was visualized using Novex AP Chromogenic Substrate (BCIP/NBT) (Invitrogen, Thermo Fisher Scientific).

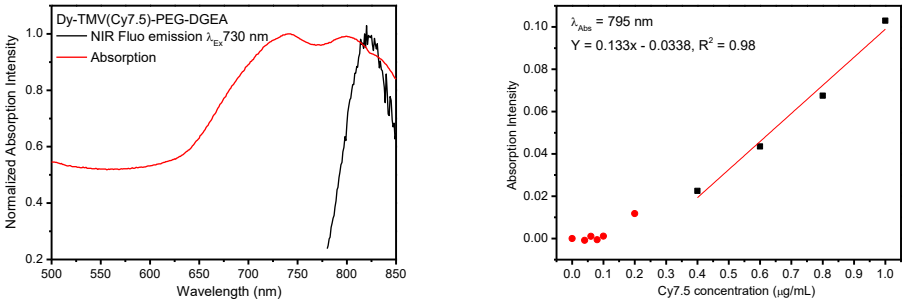

Figure S2. The absorption and NIRF emission spectrum of Dy-Cy7.5-TMV-DGEA nanoparticles in PBS (left) and the absorption of the same nanoparticles as a function of Cy7.5 concentration (right).

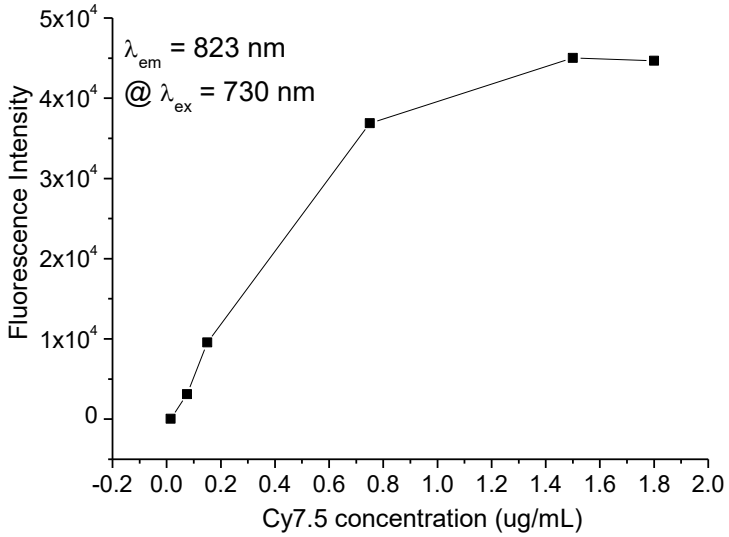

Figure S3. The NIRF intensity of Cy7.5 dye at different concentrations. The intensity of fluorescence was quenched as the concentration increased above 1.5 μg/mL (1.95 nmol/mL).

Table 1. Comparison of $r_{1,2}$ relaxivity of Dy^{3+}-based nanoparticles and the current clinical T_2 contrast agents for MRI

Contrast agents	Surface coating	Size (nm)	HD (nm)	r_2 ($mM^{-1}s^{-1}$)	r_1 ($mM^{-1}s^{-1}$)	r_2 / r_1	Field (T)	Ref.
Dy-TMV	PEG2k	300 x 18		399	2.5	160	9.4	This work
Dy-TMV	PEG2k	300 x 18		326	2.1	155	7	This work
$NaDyF_4$ NP	PMAO-PEG	20.3	33.7	101	0.33	306	9.4	1
$NaDyF_4$:Tb^{3+}	CTAB	35		22.325			7	2
Dy_2O_3	Dextran	70		190			7	3
Dy_2O_3	D-glu. acid	2.9		40	0.16	250	3	4
Dy-fullerenol [5]				20			9.4	6
Dy-DTPA-PcHexPh2				3	0.11	27	7	7
Combidex (Fe_3O_4)	Dextran	5.85	35	60	10	6	1.5	8
Feridex (Fe_3O_4, γ-Fe_2O_3)	Dextran	4.96	160	93	4.1	22	3	9
Resovist (Fe_3O_4)	carboxydextran	4	60	143	4.6	31	3	9

HD: hydrodynamic diameter, D-glu. acid: D-glucuronic acid; DTPA-$PcHexPh_2$: 2-(R)-[(4,4-diphenylcyclohexyl)phosphonooxymethyl]-diethylenetriamine-N,N,N',N''N''-pentaacetic acid. CTAB: cetyltrimethylammonium bromide.

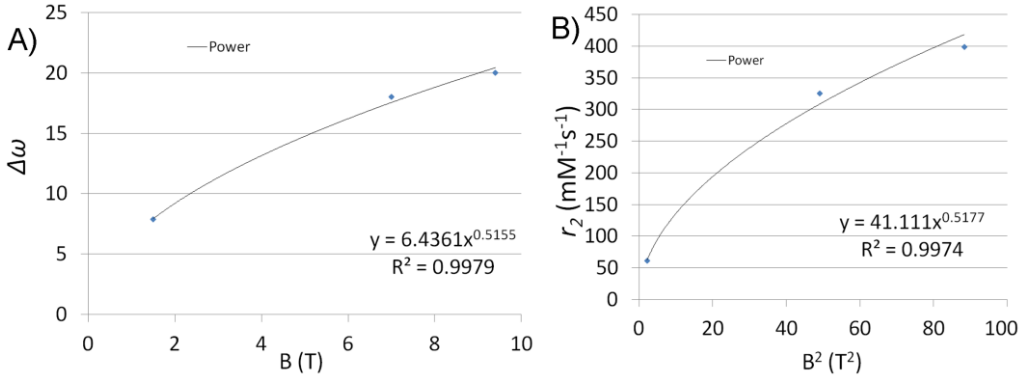

Figure S4. (A) The Δω as a function of the magnetic field B, and (B) r_2 as a function of the square of magnetic field (B^2).

Binding Affinity Measurements:

The affinity constant (K_d) of Dy-Cy7.5-TMV-DGEA nanoparticles to PC-3 cells was determined as follows: PC-3 cells (2×10^5 cells per well in 24-well plates in triplicate) were incubated with 0–600 μg/mL Dy-Cy7.5-TMV-DGEA nanoparticles in cell culture medium at 37 ^oC for 2 hours. Nonspecific binding was determined by adding non-targeted Dy-Cy7.5-TMV-mPEG nanoparticles at the same condition. Cells were washed with cold PBS buffer, and fluorescence emission was recorded using the IVIS 200 small-animal imaging system (Xenogen, Alameda, CA, USA) and normalized to photons per second per centimeter squared per steradian ($p/s/cm^2/sr$). Specific binding was calculated as the difference between total binding and nonspecific binding. Data represent the mean±SD of triplicates. The K_d was determined by nonlinear regression analysis using GraphPad Prism software. The K_d of Dy-Cy7.5-TMV-DGEA to PC-3 cells was 71.5 nM by nonlinear regression analysis;

this follows the same rank order of reported affinities of anti-prostate specific membrane antigen (PSMA) monoclonal antibodies (35.6-46.5 nM).[10]

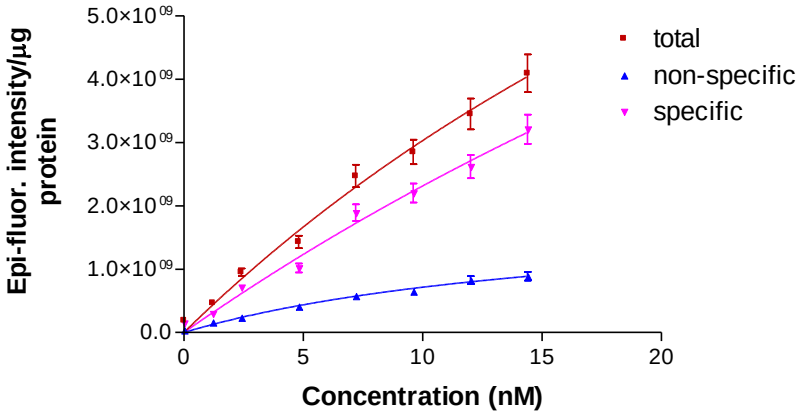

Figure S5. Binding affinity profiles of Dy-Cy7.5-TMV-DGEA nanoparticles to prostate cancer PC-3 cell lines. The K_d of Dy-Cy7.5-TMV-DGEA to PC-3 cells was 71.5 nM by nonlinear regression analysis.

Transverse relaxivity r_2 of Dy^{3+}

As previously reported,[3, 11] the transverse relaxation of paramagnetic Ln^{3+} ions is modulated by two correlation times: the diffusion correlation time, τ_D ($\tau_D = r^2/D$, where D = 3.0813×10^{-9} m^2s^{-1}, the diffusion coefficient of water at 37°C), and the static correlation time, $1/\Delta\omega$, where r is the radius of the nanoparticles and $\Delta\omega$ is the difference in Larmor frequency at the nanoparticles surface and that at infinity. For small nanoparticle sizes ($\tau_D \ll 1/\Delta\omega$), provided that diffusion is not disturbed by the refocusing pluses ($\tau_D \ll \tau_{CP}$), where τ_{CP} is the half the time interval between two successive refocusing pluses, the relaxivity is dependent on τ_D and can be described by out-sphere theory. This transverse relaxivity r_2 is given as

$$r_2 = \frac{1}{2}\nu\Delta\omega^2\tau_D$$

Where ν is the volume fraction of the nanoparticles.

Transverse Curie relaxivity (r_2^C) of Dy^{3+}

As previously reported,[3, 11-12] the relaxation enhancement of water protons is the sum of the outer-sphere and inner-sphere relaxations. The inner-sphere relaxation mechanism is associated with water molecules directly bonding to paramagnetic ions, whereas no bonding is needed for outer-sphere relaxation. Due to the strongly hydrophilic nature of the TMV coat protein and PEG-peptide coatings, we can assume that the experimental proton relaxation of the nanoparticles is mainly dominated by the outer-sphere mechanism.

The outer-sphere contribution of the Curie is given as follows:

$$\mathrm{R_{2OS}^{C}} = \frac{1}{\mathrm{T_{2OS}^{C}}} = \frac{16\pi}{45000}\left(\frac{\mu_0}{4\pi}\right)^2 \gamma_\mathrm{I}^2\mu_\mathrm{B}^2 g_\mathrm{J}^2 \mathrm{N_A}\frac{[\mathrm{Dy}]}{\mathrm{aD}}\mu_\mathrm{C}^2 \times [3\mathrm{J_A}(\sqrt{2\omega_\mathrm{I}\tau_\mathrm{D}}) + 4\mathrm{J_A}(0)] \qquad \text{(eq 1)}$$

where μ_0 is the permeability of a vacuum, γ_I is the proton gyromagnetic ratio, μ_B is the Bohr magneton, g_J is Landé factor of Dy^{3+}, N_A is the Avogadro constant, [Dy] is the molar concentration of the Dy^{3+} ion, D is the water diffusion coefficient, μ_C is the Curie moment, J_A is Ayant's spectral density function, and ω_I is the angular proton Lamor frequency ($\omega_\mathrm{I} = \gamma_\mathrm{I}\mathrm{B}$).

The Curie moment μ_C can then be expressed as follows:

$\mu_C = \frac{\mu_{eff}^2 B}{3k_B T}$, where $\mu_{eff} = g_J \mu_B \sqrt{J(J+1)}$ (eq 2)

where B is the magnetic field, J is the quantum number of the total spin, k_B is the Boltzmann constant and T is the absolute temperature.

Ayant's spectral density function (J_A) can be expressed as follows:

$$J_A(u) = \frac{1+\frac{5u}{8}+\frac{u^2}{8}}{1+u+\frac{u^2}{2}+\frac{u^3}{6}+\frac{4u^4}{81}+\frac{u^5}{81}+\frac{u^6}{648}}, \text{ where } u = \sqrt{2\omega_I \tau_D} \quad \text{(eq 3)}$$

By using Equations 1–3, the Curie relaxivity r_2^C can be given as follows:

$$r_2^C = \frac{R_{2OS}^C}{[Dy]} = \frac{16\pi}{45000}\left(\frac{\mu_0}{4\pi}\right)^2 \left(\frac{\mu_{eff}^2}{3k_B T}\right)^2 \gamma_I^2 \mu_B^2 g_J^2 N_A \frac{1}{D^{\frac{3}{2}}} \frac{B^2}{\sqrt{\tau_D}} \times [3J_A(\sqrt{2\omega_I \tau_D}) + 4J_A(0)] \quad \text{(eq 4)}$$

where the Curie constant (C_0) and the function of translational correlation time $\varphi(\tau_D)$ can be given as follows:

$$C_0 = \frac{16\pi}{45000}\left(\frac{\mu_0}{4\pi}\right)^2 \left(\frac{\mu_{eff}^2}{3k_B T}\right)^2 \gamma_I^2 \mu_B^2 g_J^2 N_A \frac{1}{D^{\frac{3}{2}}} \quad \text{(eq 5)}$$

$$\varphi(\tau_D) = \frac{3J_A(\sqrt{2\omega_I \tau_D})+4J_A(0)}{\sqrt{\tau_D}} \quad \text{(eq 6)}$$

Then, r_2^C can be expressed as:

$$r_2^C = C_0 B^2 \varphi(\tau_D)$$

The r_2 value is proportional to the square of magnetic field (B^2).

References:

1. Das, G. K.; Johnson, N. J. J.; Cramen, J.; Blasiak, B.; Latta, P.; Tomanek, B.; van Veggel, F. C. J. M., $NaDyF_4$ Nanoparticles as T_2 Contrast Agents for Ultrahigh Field Magnetic Resonance Imaging. *J. Phys. Chem. Lett.* **2012,** *3*, 524-529.

2. Zhang, Y.; Vijayaragavan, V.; Das, G. K.; Bhakoo, K. K.; Tan, T. T. Y., Single-Phase $NaDyF_4:Tb^{3+}$ Nanocrystals as Multifunctional Contrast Agents in High-Field Magnetic Resonance and Optical Imaging. *Eur. J. Inorg. Chem.* **2012,** *2012*, 2044-2048.

3. Norek, M.; Kampert, E.; Zeitler, U.; Peters, J. A., Tuning of the Size of Dy_2O_3 Nanoparticles for Optimal Performance as an MRI Contrast Agent. *J. Am. Chem. Soc.* **2008,** *130*, 5335-5340.

4. Kattel, K.; Park, J. Y.; Xu, W.; Kim, H. G.; Lee, E. J.; Bony, B. A.; Heo, W. C.; Lee, J. J.; Jin, S.; Baeck, J. S.; Chang, Y.; Kim, T. J.; Bae, J. E.; Chae, K. S.; Lee, G. H., A Facile Synthesis, *In vitro* and *In vivo* MR Studies of d-Glucuronic Acid-Coated Ultrasmall Ln_2O_3 (Ln = Eu, Gd, Dy, Ho, and Er) Nanoparticles as a New Potential MRI Contrast Agent. *ACS Appl. Mater. Interfaces* **2011,** *3*, 3325-3334.

5. Afshar-Oromieh, A.; Haberkorn, U.; Schlemmer, H. P.; Fenchel, M.; Eder, M.; Eisenhut, M.; Hadaschik, B. A.; Kopp-Schneider, A.; Röthke, M., Comparison of PET/CT and PET/MRI hybrid systems using a 68Ga-labelled PSMA ligand for the diagnosis of recurrent prostate cancer: initial experience. *Eur. J. Nucl. Med. Mol. Imaging* **2013,** *41*, 887-897.

6. Kato, H.; Kanazawa, Y.; Okumura, M.; Taninaka, A.; Yokawa, T.; Shinohara, H., Lanthanoid Endohedral Metallofullerenols for MRI Contrast Agents. *J. Am. Chem. Soc.* **2003,** *125*, 4391-4397.

7. Caravan, P.; Greenfield, M. T.; Bulte, J. W. M., Molecular Factors That Determine Curie Spin Relaxation in Dysprosium Complexes. *Magn. Reson. Med.* **2001,** *46*,

917-922.

8. Wang, Y.-X. J., Superparamagnetic iron oxide based MRI contrast agents: Current status of clinical application. *Quant. Imaging Med. Surg.* **2011,** *1*, 35-40.

9. Rohrer, M.; Bauer, H.; Mintorovitch, J.; Requardt, M.; Weinmann, H.-J., Comparison of Magnetic Properties of MRI Contrast Media Solutions at Different Magnetic Field Strengths. *Invest. Radiol.* **2005,** *40*, 715-724.

10. Wang, X.; Ma, D.; Olson, W. C.; Heston, W. D. W., *In Vitro* and *In Vivo* Responses of Advanced Prostate Tumors to PSMA ADC, an Auristatin-Conjugated Antibody to Prostate-Specific Membrane Antigen. *Molecular Cancer Therapeutics* **2011,** *10*, 1728-1739.

11. Norek, M.; Peters, J. A., MRI Contrast Agents Based on Dysprosium or Holmium. *Prog. Nucl. Magn. Reson. Spectrosc.* **2011,** *59*, 64-82.

12. Ni, D.; Zhang, J.; Bu, W.; Zhang, C.; Yao, Z.; Xing, H.; Wang, J.; Duan, F.; Liu, Y.; Fan, W.; Feng, X.; Shi, J., PEGylated $NaHoF_4$ Nanoparticles as Contrast Agents for Both X-Ray Computed Tomography and Ultra-High Field Magnetic Resonance Imaging. *Biomaterials* **2016,** *76*, 218-225.